MOLECULAR AND CELLULAR BIOLOGY, Dec. 2007, p. 8648–8657 Vol. 27, No. 24
0270-7306/07/$08.00+0 doi:10.1128/MCB.00866-07

An EGR2/CITED1 Transcription Factor Complex and the 14-3-3σ Tumor Suppressor Are Involved in Regulating ErbB2 Expression in a Transgenic-Mouse Model of Human Breast Cancer▽

Rachelle L. Dillon,[1,2] Stephen T. Brown,[4] Chen Ling,[1,2] Toshishiro Shioda,[5] and William J. Muller[1,2,3]*

Molecular Oncology Group, McGill University Health Center,[1] and Departments of Biochemistry[2] and Medicine,[3] McGill University, Montreal, Quebec, Canada; Department of Biology, McMaster University, Hamilton, Ontario, Canada[4]; and Department of Tumor Biology, Massachusetts General Hospital Center for Cancer Research, Charlestown, Massachusetts[5]

Received 16 May 2007/Returned for modification 19 July 2007/Accepted 2 October 2007

Amplification and elevated expression of the ErbB2 receptor tyrosine kinase occurs in 20% of human breast cancers and is associated with a poor prognosis. We have previously demonstrated that mammary tissue-specific expression of activated ErbB2 under the control of its endogenous promoter results in mammary tumor formation. Tumor development was associated with amplification and overexpression of ErbB2 at both the transcript and protein levels. Here we demonstrate that the EGR2/Krox20 transcription factor and its coactivator CITED1 are coordinately upregulated during ErbB2 tumor induction. We have identified an EGR2 binding site in the *erbB2* promoter and demonstrated by chromatin immunoprecipitation assays that EGR2 and CITED1 associate specifically with this region of the promoter. EGR2 and CITED1 were shown to associate, and expression from an *erbB2* promoter-reporter construct was stimulated by EGR2 and was further enhanced by CITED1 coexpression. Furthermore, expression of the 14-3-3σ tumor suppressor led to down-regulation of ErbB2 protein levels and relocalization of EGR2 from the nucleus to the cytoplasm. Taken together, these observations suggest that, in addition to an increased gene copy number and upregulation of EGR2 and CITED1, an elevated *erbB2* transcript level involves the loss of 14-3-3σ, which sequesters a key transcriptional regulator of the *erbB2* promoter.

ErbB2 (HER2, Neu) belongs to the epidermal growth factor receptor (EGFR) family of receptor tyrosine kinases (11, 21). Overexpression of ErbB2 has been implicated in 20 to 30% of primary breast cancers and correlates with a poor prognosis and clinical outcome (22, 42, 43). ErbB2 overexpression in human breast cancer has been shown to occur through genomic amplification (23); however, overexpression has also been observed for single-copy genes (24). In addition, ErbB2-overexpressing human breast cancer cell lines have been demonstrated to have higher *erbB2* transcript levels per gene copy number compared to cell lines expressing low levels of ErbB2 (20, 26). In contrast to the rodent promoters, the human *erbB2* promoter has been analyzed more extensively and the proximal 0.22 kb is thought to contain the most positive-acting elements. Several transcription factors that regulate expression from this region of the promoter have been identified. Transcription factor AP-2 was shown to activate *erbB2* expression (7), and this activity was attributable to the AP-2α, -β, and -γ family members (6). In addition, an Ets binding site positioned between the two transcriptional start sites, located at positions −69 and +1, has been shown to be bound by three Ets family members, namely, PEA3, ESX/Elf-3, and Elf-1, resulting in activation from the *erbB2* promoter (5, 9, 39).

The importance of ErbB2 in mammary tumor development has been demonstrated through the use of transgenic-mouse models expressing various constitutively active forms of the receptor in the mammary epithelium by use of the mouse mammary tumor virus (MMTV) promoter-enhancer (8, 15, 41). More recently, we have shown that the expression of activated ErbB2 from the endogenous *erbB2* promoter also leads to mammary tumor formation. Tumor progression in this mouse model was associated with a dramatic elevation of both ErbB2 protein and transcript levels. Elevated ErbB2 expression was further correlated with genomic amplification of the activated allele (3). Reminiscent of the findings obtained with human mammary carcinoma cell lines, the significant upregulation of the ErbB2 protein and transcript in these mammary tumors cannot simply be attributable to amplification of the activated *erbB2* allele. In addition to genomic amplification of *erbB2*, mammary tumors that arise exhibit frequent loss of the distal end of chromosome 4. Subsequent fine mapping of this region by comparative genomic hybridization-bacterial artificial chromosome array analyses revealed that the putative tumor suppressor 14-3-3σ, which mapped to this interval, was frequently lost during tumor induction in this mouse model (17).

One possible explanation for the dramatic upregulation of activated ErbB2 expression is that the levels of key transcription factors involved in regulating the *erbB2* promoter have been altered. Comparison of the gene expression profile of tumors derived from transgenic mice expressing activated ErbB2 under the transcriptional control of the *erbB2* promoter

* Corresponding author. Mailing address: Molecular Oncology Group, Royal Victoria Hospital, Room H5.63A, 687 Pine Avenue West, Montreal, Quebec H3A 1A1, Canada. Phone: (514) 934-1934, ext. 36384. Fax: (514) 843-1478. E-mail: william.muller@mcgill.ca.

▽ Published ahead of print on 15 October 2007.

with mice expressing activated ErbB2 from the MMTV promoter identified a number of transcription factors that were differentially expressed (1). In this study, we have explored the role of two of these candidate transcription factors, EGR2 and CITED1, which were both upregulated in tumors derived from mice expressing activated ErbB2 from the endogenous promoter.

EGR2/Krox20 is a zinc finger transcription factor belonging to the early growth response (EGR) family. The EGR family members are characterized by a DNA-binding domain consisting of three zinc finger motifs which bind to 9-bp GC-rich DNA sequences. EGR2 functional studies have been conducted most extensively in the mouse nervous system. In the central nervous system, EGR2 has been shown to directly regulate the genes for Hoxb2 and Hoxa2 (36, 37), as well as the gene for the EphA4 tyrosine kinase (46), in rhombomeres 3 and 5 of the developing hindbrain. EGR2 has also been shown to activate the expression of *Hoxb3* in rhombomere 5 (30). A negative role for EGR2 in regulating the expression of another Hox-encoding gene, *Hoxb1*, has been reported, although in this case the regulation is indirect in that EGR2 antagonizes the positive regulatory factor PIASxβ (13). Other studies have revealed a role for EGR2 in the peripheral nervous system, notably in Schwann cells, where it has been demonstrated that EGR2 regulates the expression of myelination-related genes, including the direct activation of *mpz* expression (27).

CITED1, a transcriptional coactivator belonging to the CITED family, was originally identified in a murine melanoma cell line and implicated in the melanogenesis process (33, 40). Members of this family of non-DNA-binding proteins contain a well conserved C-terminal acidic domain that accounts for their strong transcriptional activating activity (40). CITED1 has been shown to interact with SMAD4 and CPB/p300, serving to enhance SMAD-mediated transcription by strengthening the link with CBP/p300 (52). It has also been demonstrated that CITED1 interacts with ERα and ERβ and through this association enhances estrogen-induced transcription (53).

Although many studies have examined the impact of *erbB2* overexpression in terms of the downstream signaling pathways, very little is known regarding the precise mechanisms by which *erbB2* overexpression occurs. Here we provide evidence that EGR2 and CITED1 function to positively regulate *erbB2* expression. We have identified an EGR2 binding site within the *erbB2* promoter and demonstrated association between EGR2 and the CITED1 transcriptional coactivator. EGR2 and CITED1 were shown to associate with the *erbB2* promoter region containing the EGR2 binding site, and both activated transcription from an *erbB2* promoter construct, in the case of CITED1 in a manner dependent on the coexpression of EGR2. Furthermore, we demonstrated that EGR2 associates with 14-3-3σ and expression of 14-3-3σ led to the sequestration of EGR2 in the cytoplasm and thus provides a means of downregulating *erbB2* levels. Collectively, the results of this study suggest that the loss of 14-3-3σ can cooperate with amplification of *erbB2* to elevate ErbB2 expression during mammary tumor progression.

MATERIALS AND METHODS

Mice. MMTV-Cre/FloxNeoNeuNT- and MMTV-activated ErbB2 mice were bred in our animal facility. All animal experiments were performed in accordance with the guidelines of the Royal Victoria Hospital Facility Animal Care Committee.

Plasmid construction. *EGR2* and *CITED1* cDNAs were prepared by reverse transcriptase PCR (RT-PCR) from RNA isolated from a KI mammary tumor and ligated into pEF6-V5/His-TOPO (Invitrogen) as a PCR product or pCMV-HA (Clontech) as an EcoRI-KpnI fragment, respectively. EGR2 cDNA was then subcloned as a BamHI/PmeI fragment into the BglII/HpaI sites of pMSCV-puro (Clontech). CITED1 cDNA was subcloned as a blunted NcoI/ClaI fragment into the HpaI site of pMSCV-puro. A 1,044-bp region of the *erbB2* promoter was cloned by PCR from DNA isolated from an FVB/n mouse, ligated into pCR2.1-TOPO (Invitrogen), and subcloned as a KpnI-XhoI fragment into the pGL3-Basic vector (Promega). Site-directed mutagenesis of the EGR2 binding site was performed with the QuikChangeXL kit from Stratagene. Mouse 14-3-3σ cDNA was a kind gift from Joe W. Gray (Ernest Orlando Berkeley National Laboratory, University of California, San Francisco) and was subsequently amplified and cloned into the BglII/HpaI site of pMSCV-hygro (Clontech). A 14-3-3ζ expression construct was a kind gift from Dihua Yu (MD Anderson Cancer Center, University of Texas, Houston). All constructs were verified by sequencing.

Cell culture and transfection. 293T and C6 cells were grown in Dulbecco modified Eagle medium (DMEM) supplemented with 10% fetal bovine serum (FBS). HS578T cells were grown in DMEM supplemented with 5% FBS. The KI mammary tumor-derived cell line TM15 was maintained in DMEM supplemented with 10% FBS and Single Quots (Clonetics). Transfections were performed with FuGENE 6 (Roche) in accordance with the manufacturer's instructions at a ratio of 3 μl of FuGENE 6 to 1 μg of DNA. TM15 cell lines expressing EGR2, CITED1, 14-3-3σ, and 14-3-3ζ were generated by retroviral infection. Following infection, resistant TM15 cells were selected with 4 μg/ml puromycin or 300 μg/ml hygromycin.

Coimmunoprecipitations. 293T cells were transfected with 2 μg of total DNA, harvested at 48 h following transfection, and lysed with modified TNE buffer (50 mM Tris [pH 8.0], 150 mM NaCl, 1% Nonidet P-40 [NP-40], 10 mM sodium fluoride, 10 mM sodium pyrophosphate, 2 mM EDTA) supplemented with 1 μg/ml leupeptin, 1 μg/ml aprotinin, and 1 mM sodium orthovanadate (Na_3VO_4). Subconfluent TM15 cells were lysed with modified TNE buffer supplemented with protease inhibitors and Na_3VO_4. Immunoprecipitations were performed overnight at 4°C with antibodies to V5 (1:500; Invitrogen or GenWay Biotech), hemagglutinin (HA; 1:500 [HA.11]; Covance), and 14-3-3σ (clone CS112-2A8 at 1:250; Upstate Biotechnology). Immunoprecipitations were then incubated for 2 h with protein G-agarose (Amersham Biosciences). The reaction products were washed with lysis buffer, and the immune complexes were resolved by sodium dodecyl sulfate-polyacrylamide gel electrophoresis (SDS-PAGE). The proteins were electrotransferred to polyvinylidene difluoride membranes, and the membranes were immunoblotted with antibodies to V5 (1:2,000; Invitrogen), EGR2 (1:1,000; Covance), and 14-3-3σ (C-18 at 1:100; Santa Cruz Biotechnology); a chicken anti-HA antibody (1:1,000; Chemicon International); and a rabbit polyclonal anti-CITED1 antibody (MG043) raised against a synthetic peptide corresponding to amino acids 154 to 168 of mouse CITED1 (1:1,000). Secondary antibodies (goat anti-mouse, goat anti-rabbit, donkey anti-goat, and rabbit anti-chicken antibodies conjugated to horseradish peroxidase [HRP]; Jackson Laboratories) were used at 1:10,000, and the proteins were visualized by enhanced chemiluminescence (ECL; Amersham Biosciences).

Tissue harvesting and analysis. Mammary tumors were excised and snap-frozen in liquid nitrogen. For protein analyses, extracts were prepared in modified TNE lysis buffer supplemented with protease inhibitors. The proteins were separated by SDS-PAGE and transferred to polyvinylidene difluoride membranes. Immunoblotting was performed with a rabbit polyclonal antibody (MG044) raised against a synthetic peptide corresponding to amino acids 354 to 368 of mouse EGR2 (1:1,000), a mouse monoclonal antibody (2H6) against full-length human CITED1 (1:1,000), and an anti-Grb2 antibody (C-23 at 1:1,000; Santa Cruz Biotechnology). Secondary antibodies conjugated to HRP were used at a 1:10,000 dilution, and the proteins were visualized by ECL. Total RNA was isolated from flash-frozen mammary tumors with the RNeasy Midi Kit (QIAGEN). Tumor tissue RNA was analyzed by RT-PCR with a LightCycler and a SYBR green I RNA amplification kit (Roche). RT-PCRs were performed in triplicate, and transcript levels were normalized to glyceraldehyde-3-phosphate dehydrogenase (GAPDH). Primer sequences were as follows: EGR2 sense, 5′-CAGGAGTGACGAAAGGAAGC-3′; EGR2 antisense, 5′-GAAGA CTGGGCAGATGGAGG-3′; CITED1 sense, 5′-CTCCTCTGGATCGACATC TCC-3′; CITED1 antisense, 5′-CTTCTGAAGCTGCATGCTGG-3′; GAPDH sense, 5′-GCAAAGTGGAGATTGTTGCC-3′; GAPDH antisense, 5′-ATTCT CGGCCTTGACTGTGC-3′.

Electrophoretic mobility shift assays. 293T cells were transfected with a V5-tagged EGR2 expression vector, and extracts were prepared at 48 h posttransfection. Gel shift probes were prepared by annealing the oligonucleotides EGR2 binding consensus F (5′-CAGCACCAAAGTGGGTGGGCGGCACCCTGTA A-3′) and R (5′-GAGTTACAGGGTGCCGCCCACCCACTTTGGTG-3′) and mutated EGR2 binding consensus F (5′-CAGCACCAAAGTGGGTGGGGGG CACCCTGTAA-3′) and R (5′-GAGTTACAGGGTGCCCCCCACCCACTTT GGTG-3′) (nucleotide substitution underlined). Annealed oligonucleotides were labeled with 5 μCi of [α-^{32}P]dCTP with Klenow and purified on a G50 Sephadex column (Amersham). Binding reactions were performed with buffer containing 20 mM HEPES (pH 7.5), 10 μM $ZnSO_4$, 2 mM dithiothreitol, 10% glycerol, 0.02 μg/μl poly(dI-dC) · poly(dI-dC), 0.1 μg/μl bovine serum albumin, 1 mM phenylmethylsulfonyl fluoride, and 60 mM KCl and incubation for 30 min at 30°C. For supershift reactions, 1 μg of anti-V5 antibody was added following the initial incubation period and the mixture was incubated for an additional 10 min at 30°C. Probe bound to protein was then separated from free probe by electrophoresis at 150 V through a 5% nondenaturing polyacrylamide (29:1) gel containing 0.5× Tris-borate-EDTA and 3% glycerol. The gels were dried and visualized by autoradiography.

Luciferase assays. Cells were seeded into six-well plates. In one assay (see Fig. 4), a total of 1,150 ng of DNA (200 ng of reporter DNA, 750 ng of effector DNA, and 200 ng of pEF1-V5/His-LacZ [Invitrogen]) was transfected. In another assay (see Fig. 5), a total of 1,400 ng of DNA (200 ng of reporter DNA; 250 ng of EGR2; 125, 250, 500, or 750 ng of CITED1, as indicated; 200 ng of pEF1-V5/His-LacZ; and empty vector to a total of 1,400 ng) was transfected. Cells were harvested at 48 h posttransfection in lysis buffer (1% Triton X-100, 15 mM $MgSO_4$, 4 mM EDTA, 1 mM dithiothreitol), and luciferase activity was determined. The luciferase activity was normalized to β-galactosidase activity. To ensure effector protein expression, all lysates were subjected to Western blot analysis.

Chromatin immunoprecipitations (ChIPs). Formaldehyde cross-linking was performed on subconfluent TM15 cells, the cells were harvested by centrifugation, and extracts were prepared in 100 μl of lysis buffer (50 mM Tris [pH 8], 1% SDS, 10 mM EDTA [pH 8], Complete Mini-EDTA protease inhibitor tablets [Roche]) for each 150-mm plate. The chromatin was sheared to fragments with average lengths of 200 to 500 bp by sonication, the supernatant was collected, and chromatin fragment length was verified by electrophoresis. For each ChIP, 150 μl of soluble chromatin was diluted with 1.2 ml of dilution buffer (20 mM Tris [pH 8.1], 1% Triton X-100, 2 mM EDTA [pH 8], 150 mM NaCl) and precleared with a 50% protein A-salmon sperm DNA slurry (Upstate Biotechnology) for 2 h at 4°C. Precleared chromatin solutions were incubated overnight with 2 μg of an antibody to V5, HA (HA.11, Covance), or EGR2 (H-220; Santa Cruz Biotechnology); a mouse monoclonal antibody (2H11) raised against full-length human CITED1; or 10 μl of antiserum to EGR2 (MG044) or CITED1 (MG043). Antibody-bound protein-DNA complexes were precipitated with a 50% protein A-salmon sperm DNA slurry for 2 h at 4°C. The immunoprecipitates were washed for 10 min each in low-salt immune complex buffer (0.1% SDS, 1% Triton X-100, 2 mM EDTA [pH 8.0], 20 mM Tris [pH 8.1], 150 mM NaCl), high-salt immune complex buffer (0.1% SDS, 1% Triton X-100, 2 mM EDTA [pH 8], 20 mM Tris [pH 8.1], 500 mM NaCl), and LiCl immune complex buffer (0.25 M LiCl, 1% NP-40, 1% Na-deoxycholate, 1 mM EDTA [pH 8], 10 mM Tris [pH 8.1]) and twice with Tris-EDTA. The chromatin was eluted, de-cross-linked, and purified on a QIAquick PCR purification column (QIAGEN) in accordance with the manufacturer's instructions. PCR was performed with primers that amplify a region containing the EGR2 binding site (positions −723 to −612; EGR2 site sense [5′-GACCCAAGTTCTGTTTCCA GC-3′] and EGR2 site antisense [5′-GTCACATAAGTGCTGTTGCC-3′]) or an upstream site (positions −2284 to −2136 of the *erbB2* gene; upstream site sense [5′-GTTGCAGTTCAACCGCTGAGG-3′] and upstream site antisense [5′-GA GCCATTGCTGGCTGTATCC-3′]) by standard PCR and quantitative PCR (Q-PCR). For Q-PCR, each reaction was done in triplicate with a LightCycler and a QuantiTect SYBR green PCR kit (QIAGEN). *n*-Fold enrichment was determined by comparing the relative amounts of specific chromatin present in the antibody-immunoprecipitated samples with the amount present in the no-antibody control following normalization for the amount of input DNA.

Immunostaining. For immunohistochemical analysis, paraffin-embedded sections were deparaffinized in three changes of xylene. Sections were heated in 10 mM sodium citrate (pH 6), followed by incubation in 3% H_2O_2 for 20 min. Samples were incubated in a primary antibody (EGR2, MGO44; CITED1, MG043) diluted 1:100 in phosphate-buffered saline (PBS)–2% bovine serum albumin (BSA) for 1 h at room temperature, washed with PBS, and then incubated for 30 min at room temperature with an HRP-conjugated secondary antibody (diluted 1:1,000 in PBS–2% BSA; Jackson Laboratories). Immunoreactivity was visualized with the DAB+ substrate chromogen system (DAKO), and the tissues were counterstained with hematoxylin. For immunofluorescent staining, cells were fixed with 2% paraformaldehyde in PBS, permeabilized in 0.5% Triton X-100 in PBS, and then washed with 100 mM glycine in PBS. Blocking was performed with IF buffer (PBS, 0.1% BSA, 0.2% Triton X-100, 0.05% Tween 20) plus 2% BSA, followed by a 1-h incubation at room temperature in a humidified chamber with primary antibodies to EGR2 (1:100; Covance), 14-3-3σ (1:100 clone CS112-2A8 [Upstate Biotechnology] and 1:100 C-18 [Santa Cruz Biotechnology]), HA (1:5,000), and ErbB2 (Ab3 at 1:100; Oncogene) diluted in IF buffer. Cells were washed in IF buffer and incubated in a humidified chamber with the appropriate Alexa-Fluor-conjugated secondary antibodies diluted in IF buffer (1:1,000; Molecular Probes) for 40 min at room temperature. The nuclei were counterstained with 4′,6′-diamidino-2-phenylindole (DAPI).

Confocal imaging. Confocal imaging was performed with an Axiovert 200 M microscope (Carl Zeiss MicroImaging, Inc.) with 100×/1.4 plan-Apochromat objectives equipped with a confocal microscope system (LSM 510 Meta confocal microscope; Carl Zeiss MicroImaging, Inc.). Image analysis was carried out with the LSM 5 image browser (Empix Imaging).

RESULTS

EGR2 and CITED1 are upregulated in MMTV-Cre/Flox-NeoNeuNT mammary tumors. We have previously shown by microarray analysis that EGR2 and CITED1 are overexpressed in mammary tumors induced by expression of activated ErbB2 under the transcriptional control of the *erbB2* promoter (herein referred to as the KI model) compared to MMTV-activated ErbB2 mammary tumors (1). To confirm the microarray results, we analyzed the mRNA and protein levels of EGR2 and CITED1 in nine independent KI and MMTV-activated ErbB2 mammary tumors. Consistent with the microarray results, a general trend was observed in a real-time RT-PCR in which EGR2 and CITED1 transcript levels were elevated in the individual KI tumors (Fig. 1A). EGR2 mRNA was elevated an average of 5-fold and CITED1 mRNA was elevated 14-fold in the KI tumors compared to the transcript levels in the MMTV-activated ErbB2 tumors. To confirm that EGR2 and CITED1 were also elevated at the protein level, mammary tumor tissue lysates were immunoblotted for EGR2 and CITED1. In agreement with the Q-RT-PCR results, the levels of both the EGR2 and CITED1 proteins were elevated in the KI mammary tumors (Fig. 1B). In the EGR2 immunoblot assays, we detected two related EGR2 isoforms that result from differential splicing (10). The results demonstrate not only that are EGR2 and CITED1 elevated at the transcript level but that this overexpression results in increased protein levels. Furthermore, immunohistochemical staining of KI tumor tissues with EGR2- and CITED1-specific antibodies revealed that both EGR2 and CITED1 are nucleus localized in the tumors (Fig. 1C and D), demonstrating that they are both present at a location where they can fulfill their function as transcriptional regulators. Taken together, these observations suggest that EGR2 and CITED1 are coordinately upregulated with ErbB2 in mammary tumors induced in the KI model.

EGR2 associates with the *erbB2* promoter. The upregulation of EGR2 expression in mammary tumors derived from mice expressing activated ErbB2 under the control of the endogenous *erbB2* promoter suggests that EGR2 may be an important transcriptional regulator of *erbB2* expression. Sequence analysis of the *erbB2* promoter revealed a potential EGR2 binding site located at positions −695 to −686 upstream of the *erbB2* transcription initiation site. A previous study examining the

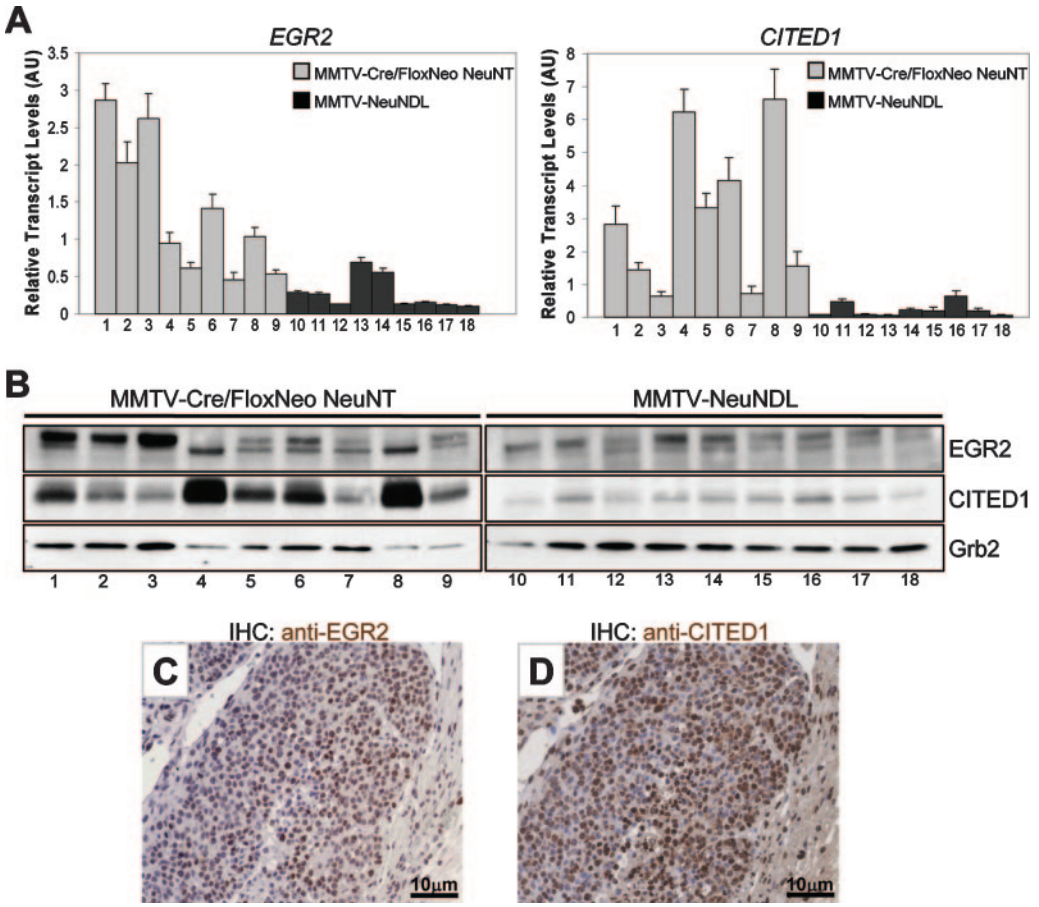

FIG. 1. EGR2 and CITED1 are overexpressed in KI mammary tumors and show nuclear localization. (A) EGR2 and CITED1 transcript levels were analyzed in KI and MMTV-activated ErbB2 mammary tumors by real-time RT-PCR. EGR2 and CITED1 transcript levels were normalized to GAPDH by the ΔΔCT method. Each relative transcript level represents the mean value of three independent amplification reactions (± the standard deviation). (B) Lysates prepared from primary mammary tumor tissues were subjected to SDS-PAGE and blotted with an EGR2 (top)- or CITED1 (middle)-specific antibody. Grb2 (bottom) was used as a control for equal loading. EGR2 (C) and CITED1 (D) expression (brown) in tissue excised from primary KI breast tumors by immunohistochemical (IHC) staining with antibodies specific to EGR2 and CITED1 is also shown. AU, arbitrary units.

binding specificity of the EGR family has shown that EGR2 can bind to a probe corresponding to this sequence (45). To directly address whether EGR2 can bind to this sequence in the context of the flanking sequences present within the *erbB2* promoter, gel shift assays were performed with a probe corresponding to positions −706 to −672 of the *erbB2* gene. When the probe was incubated with EGR2-transfected 293T lysates, a retarded complex was detected (Fig. 2A, lane 2). The presence of EGR2 in this complex was confirmed by the supershift observed upon the addition of a V5-specific antibody to tagged EGR2 (Fig. 2A, lane 3). Furthermore, this interaction could be eliminated upon the addition of an unlabeled competitor probe but not upon the addition of a large excess of a nonspecific competitor (Fig. 2A, compare lanes 4 and 5 to lane 6). To further substantiate the specificity of this interaction, the use of a probe containing a single base pair change of C to G at position 8 of the EGR2 binding consensus eliminated EGR2 binding (Fig. 2B, lanes 5 and 6). The use of the mutated probe still resulted in a shifted complex, likely corresponding to other DNA-binding factors that do not require the intact EGR2 consensus sequence. As the protein source used in this assay was the total lysate of 293T cells, a variety of other DNA-binding proteins were present in the reaction mixtures. Indeed, this complex was not supershifted when incubated with a V5-specific antibody to tagged EGR2 (Fig. 2B, lane 6), arguing that EGR2 is not present in the complex associated with the mutated probe.

To establish whether EGR2 interacts with the endogenous *erbB2* promoter, a cell line derived from a KI tumor (TM15) was generated to stably express V5-tagged EGR2 and ChIP experiments were conducted. DNA from the immunoprecipitated complexes was amplified with primers corresponding to positions −723 to −612 of the *erbB2* gene, where the EGR2 binding site is located, or with primers specific to a control upstream region. The V5 immunoprecipitates resulted in a product for the EGR2 binding region of the *erbB2* promoter (Fig. 2D, top), whereas no product was observed for the upstream control (Fig. 2D, bottom). To further substantiate this binding, the ChIPs were repeated with the parental TM15 cell line without expression of exogenous EGR2. Upon immunoprecipitation of endogenous EGR2, chromatin fragments containing the EGR2 binding site in the *erbB2* promoter were again present in the isolated chromatin (Fig. 2E), demonstrat-

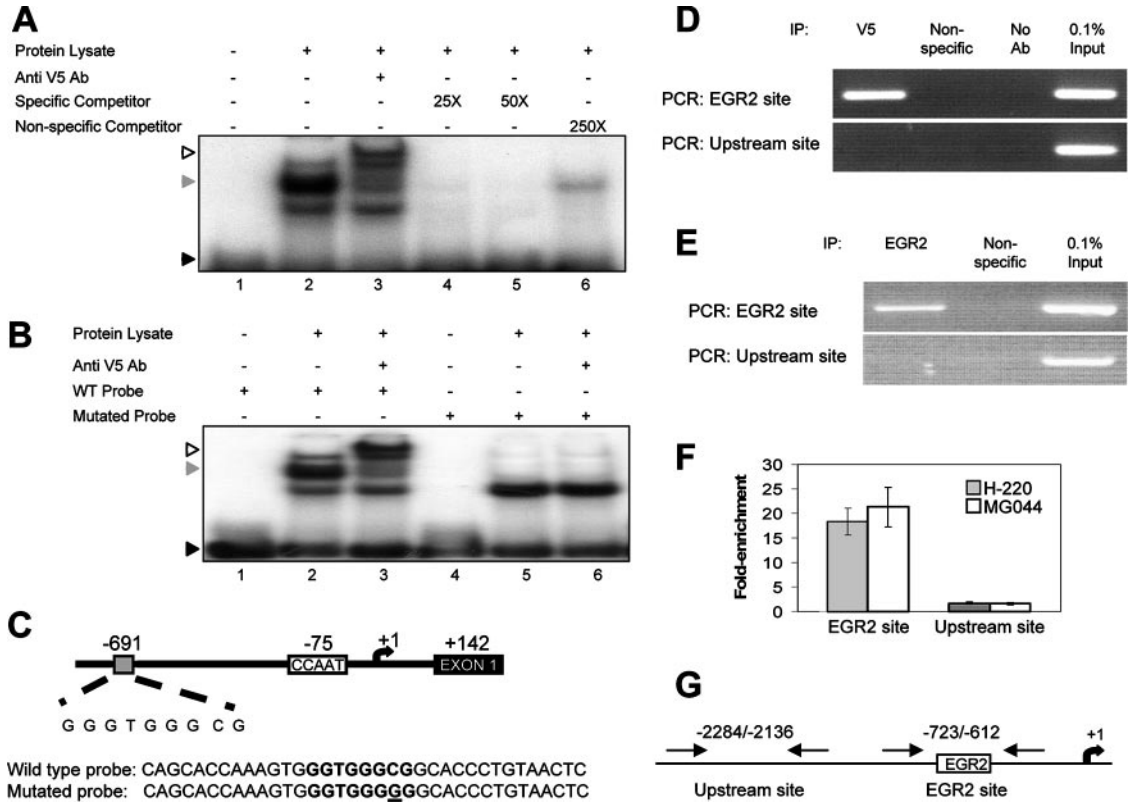

FIG. 2. EGR2 binds to a probe corresponding to a region of the *erbB2* promoter and associates with the *erbB2* promoter in vivo. (A) Lysates of 293T cells transfected with V5-tagged EGR2 were incubated with a radiolabeled probe corresponding to positions −706 to −675 of the *erbB2* promoter (lanes 2 to 6). Anti-V5 antibody (Ab) (lane 3), an unlabeled specific competitor (lanes 4 and 5), or a nonspecific competitor (lane 6) was added. (B) A probe with a single base pair substitution (lanes 4 to 6) was used. Black, gray, and white arrowheads represent free probe, shift, and supershift, respectively. WT, wild type. (C) Diagrammatic representation of the probes used. The EGR2 binding site is in bold, and the mutated oligonucleotide is underlined. (D) Chromatin from a KI mammary tumor-derived cell line expressing V5-EGR2 was immunoprecipitated (IP) with a V5-specific antibody, a nonspecific antibody, or a no-antibody control. Chromatin was amplified with primers to the EGR2 binding site within the *erbB2* gene (positions −723 to −612) or an upstream site (positions −2284 to −2136). (E) Endogenous EGR2 was immunoprecipitated from KI mammary tumor cells with an antibody directed to mouse EGR2 (Covance) and the associated chromatin amplified with the primers described for panel D. (F) Q-PCR of EGR2-associated chromatin. *n*-Fold enrichment represents the amount of chromatin corresponding to the amplified region with respect to the product obtained with the no-antibody control following normalization for input levels. Each result shown is the mean value obtained in three amplification reactions performed for two independent immunoprecipitations (± the standard deviation). (G) Diagrammatic representation of the primers used.

ing that this association occurs in a physiological context. The chromatin associated with endogenous EGR2 in ChIP assays was also analyzed by Q-PCR, which demonstrated 18.3- and 21.4-fold enrichment of chromatin representing the EGR2 binding region with two different EGR2 antibodies compared to the amount of corresponding chromatin isolated with the no-antibody control (Fig. 2F). In contrast, no enrichment of chromatin corresponding to the upstream control region of the *erbB2* gene was observed (Fig. 2F).

EGR2 activates transcription from the *erbB2* promoter. To determine whether EGR2 binding has a direct effect on transcription from the *erbB2* promoter, an approximately 1-kb region of the mouse *erbB2* promoter (positions −1225 to −182) containing the EGR2 binding site was cloned into a luciferase reporter plasmid (pGL3-wt-*erbB2*). Because previous studies have shown that erbB2 is expressed in the glial cell compartment (38), we initially tested the *erbB2* promoter construct in C6 glioblastoma cells. Transfection of the *erbB2* promoter-reporter plasmid into rat C6 glioma cells resulted in an increase in luciferase activity compared to that of the reporter plasmid lacking a promoter (Fig. 3A). This suggests that endogenous transcription factors within C6 cells are capable of activating transcription from the *erbB2* promoter construct. However, cotransfection of an EGR2 expression plasmid with the *erbB2* promoter-reporter construct resulted in an additional threefold increase in luciferase activity (Fig. 3A). This activation suggests that EGR2 plays a positive role in regulating *erbB2* expression. To confirm the necessity of a functional EGR2 binding site, an *erbB2* promoter luciferase construct containing the single base pair substitution in the EGR2 binding site that was shown to ablate EGR2 binding in the gel shift assays described above was used (pGL3-mutated-*erbB2*). In the absence of exogenous EGR2, similar basal luciferase activity levels were observed. However, in contrast to the wild-type *erbB2* promoter construct, cotransfection of EGR2 with the mutated reporter plasmid did not result in an increase in transcriptional activation (Fig. 3A). This suggests that the identified EGR2 binding site is indeed the site by which EGR2

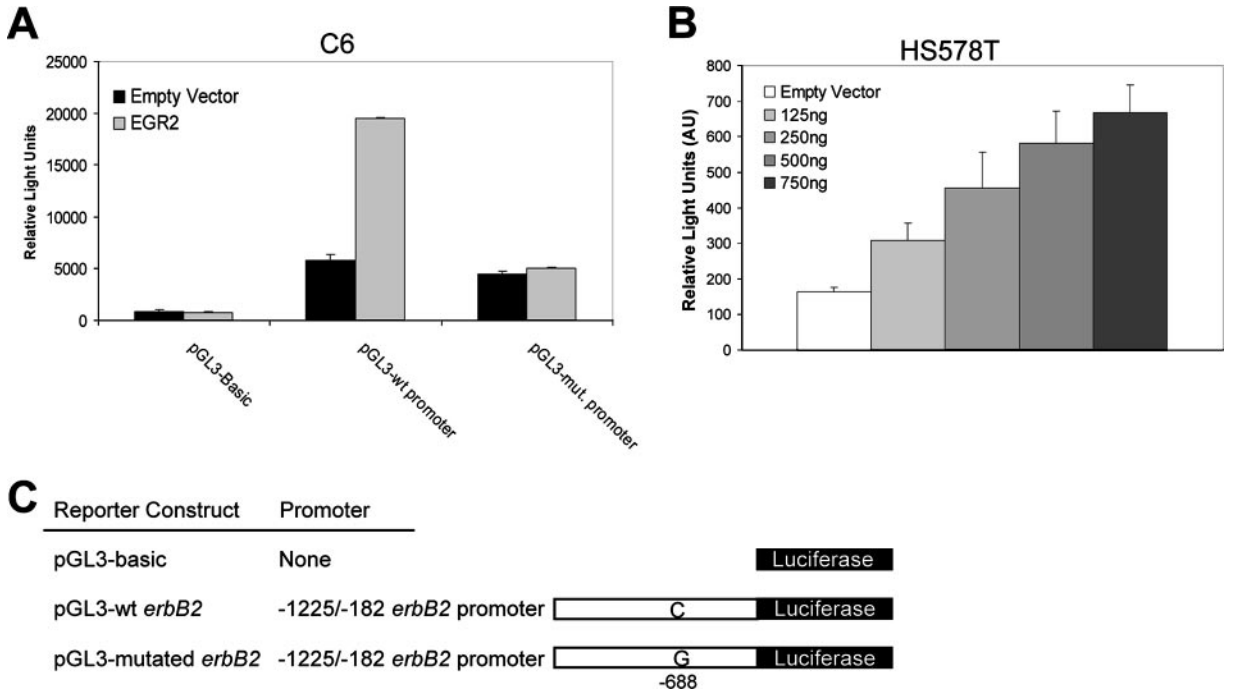

FIG. 3. EGR2 activates transcription from the *erbB2* promoter. (A) C6 cells were cotransfected with 200 ng of a reporter construct containing no promoter (pgL3-basic), the −1225 to −182 region of the *erbB2* promoter (pGL3-wt promoter), or the same region containing a mutated EGR2 binding site (pGL3-mut. promoter) and 750 ng of empty vector or EGR2 expression plasmid as indicated. Cytoplasmic extracts were prepared, and luciferase activity was measured. (B) HS578T cells were cotransfected with 200 ng of the pGL3-wt promoter construct and empty vector or EGR2 expression vector in the amounts indicated. Cytoplasmic extracts were assayed for luciferase activity. Luciferase activity is shown as relative light units normalized to β-galactosidase activity and is the mean result of three separate experiments with triplicate wells (± the standard deviation). AU, arbitrary units. (C) Diagrammatic representation of the reporter constructs used with the EGR2 binding site mutation indicated.

mediates its transcriptional activating effect from the region of the *erbB2* promoter used in these assays. The ability of EGR2 to activate transcription from the *erbB2* promoter was further validated in a human breast carcinoma cell line, HS578T. Consistent with the results obtained with the C6 glioblastoma cell line, EGR2 also activated transcription from the *erbB2* promoter construct in HS578T cells, and this occurred in a dose-dependent manner (Fig. 3B). These results argue that the observed binding of EGR2 to the *erbB2* promoter is directly involved in the transcriptional upregulation of *erbB2*.

CITED1 associates with EGR2 and the *erbB2* promoter and enhances EGR2-mediated transcriptional activation. In addition to elevated expression of EGR2, CITED1 has been previously shown to be upregulated in KI tumors (1). Given that CITED1 has been described as a potent transcriptional coactivator that associates with transcription factors (40, 52, 53), we examined the ability of CITED1 to interact with EGR2. With lysates of EGR2- and CITED1-cotransfected 293T cells, we detected V5-tagged EGR2 in HA immunoprecipitates for tagged CITED1 (Fig. 4A, top). This interaction was confirmed by performing the reciprocal immunoprecipitation in which V5 immunoprecipitates were immunoblotted for CITED1 (Fig. 4A, bottom). We then proceeded to examine what effect this had on transcription from the *erbB2* promoter. HS578T cells cotransfected with an *erbB2* promoter-luciferase construct and increasing amounts of a CITED1 expression plasmid showed no differences in luciferase activity (Fig. 4B). However, when cells were cotransfected with EGR2, increasing amounts of CITED1 led to a coordinated increase in activation (Fig. 4B). These observations suggest that CITED1 can potentiate EGR2-mediated transcriptional activation from the *erbB2* promoter. Again, this activation was dependent on the presence of a functional EGR2 binding site, whereby the use of the mutated *erbB2* promoter construct in which the EGR2 binding site is mutated showed no increase in transcriptional activation (Fig. 4B). Given that CITED1 can associate with EGR2 and affect transcription from the *erbB2* promoter in an EGR2-dependent manner, we proceeded to examine whether CITED1 associates with the EGR2 binding site region of the *erbB2* promoter. To accomplish this, we generated a TM15 cell line stably expressing HA-tagged CITED1 and performed ChIP assays. An HA-specific antibody was able to precipitate the −723 to −612 region of the *erbB2* promoter, whereas this chromatin was not detected in immunoprecipitates with a nonspecific antibody or in a no-antibody control (Fig. 4C). Furthermore, the upstream control region of the *erbB2* promoter was not detected in the CITED1 immunoprecipitates (Fig. 4C). To validate this association, the ChIPs were performed with the parental TM15 cell line and immunoprecipitation for endogenous CITED1 was performed. Again, we were able to confirm that CITED1 associates with the *erbB2* promoter region at which EGR2 binding was demonstrated (Fig. 4D). We further validated the standard PCR results by performing Q-PCR on chromatin eluted in ChIP assays with the same EGR2 binding site and upstream control primers. From this quantification, we observed 4.5- and 10.0-fold enrichments of the EGR2 binding site region of the *erbB2* promoter complexed with CITED1 with two separate CITED1 antibodies

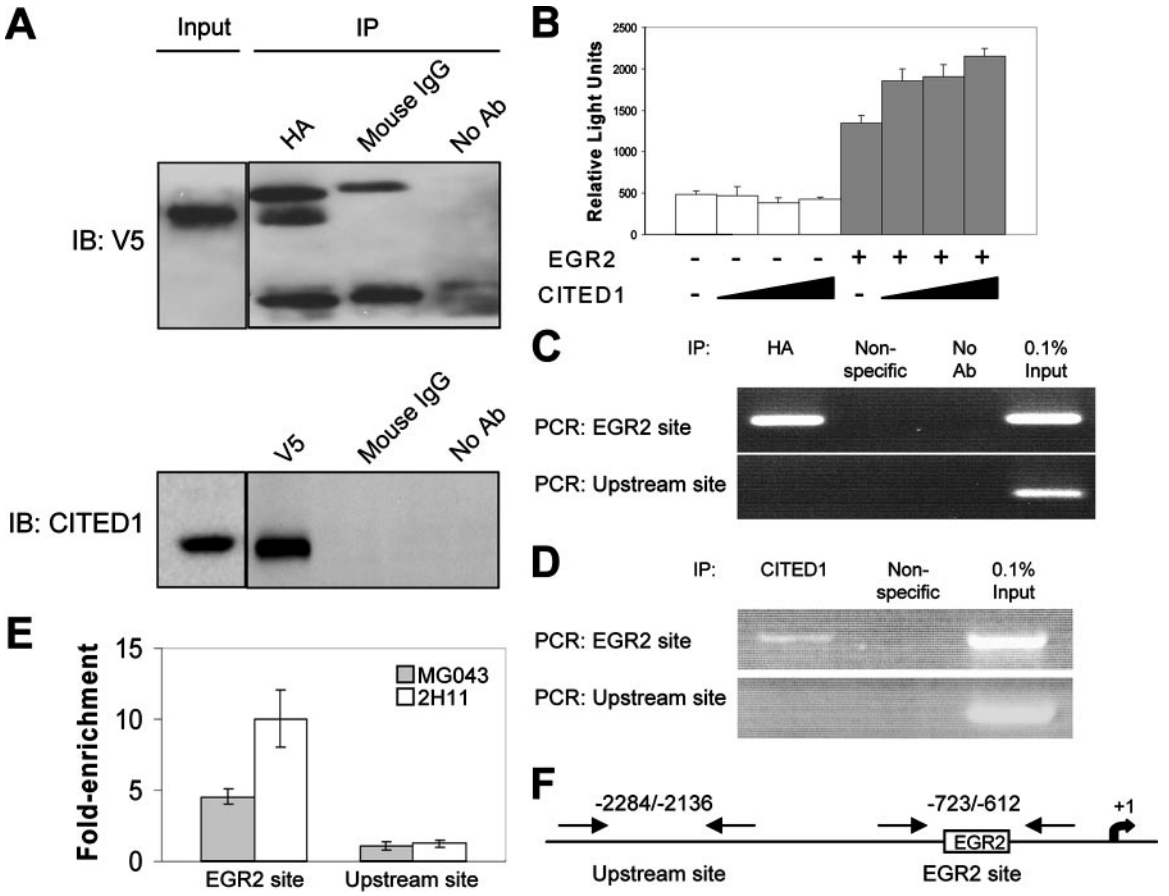

FIG. 4. CITED1 interacts with EGR2 and enhances transcription from the *erbB2* promoter. (A) Extracts of 293T cells cotransfected with V5-EGR2 and HA-CITED1 were immunoprecipitated (IP) with an anti-HA antibody (Ab) or a control antibody, and the proteins were separated by SDS-PAGE. Membranes were probed with an anti-V5 antibody to detect EGR2 (top). The same lysates were precipitated with an anti-V5 antibody, and the isolated proteins were immunoblotted (IB) for CITED1 (bottom). The amount of input lysate shown is 5% of the total protein used in the immunoprecipitations. (B) HS578T cells were cotransfected with 200 ng of the wild-type *erbB2* promoter-reporter construct described in the legend to Fig. 3 and an empty vector or an EGR2 expression vector (250 ng) and increasing amounts of a CITED1 vector (0, 250, 500, or 750 ng). Cytoplasmic extracts were assayed for luciferase activity. (C) ChIP with an HA-tagged CITED1-infected KI mammary tumor-derived cell line. Eluted chromatin was amplified with primers to the EGR2 binding site within the *erbB2* promoter or to an upstream control site. (D) Chromatin associated with endogenous CITED1 in the KI tumor-derived cell line was isolated by immunoprecipitation with an antibody raised against full-length human CITED1 (2H11) and amplified as described for panel C. (E) Q-PCR of chromatin associated with endogenous CITED1. Fold enrichment represents the amount of chromatin corresponding to the −723 to −612 region of the *erbB2* promoter compared to the no-antibody control following normalization for input levels. Each result shown is the mean value obtained in three separate amplification reactions for two independent immunoprecipitations (± the standard deviation). (F) Diagrammatic representation of the primers used.

compared to the no-antibody control (Fig. 4E). Moreover, no enrichment was observed for chromatin corresponding to the upstream control region (Fig. 4E). Taken together, these observations argue that CITED1 is present within an EGR2-containing complex which is capable of associating with the *erbB2* promoter.

14-3-3σ overexpression leads to an altered subcellular localization of EGR2 and a decrease in ErbB2 levels. Given the importance of the nuclear localization of EGR2, a potential mechanism of regulating EGR2-mediated activation of target genes is sequestration into the cytoplasm. Scansite analysis of the EGR2 protein sequence revealed a potential 14-3-3 binding site containing the consensus RXX[pS]XP, surrounding serine 376 of mouse EGR2. Of the 14-3-3 protein family, the 14-3-3σ isoform was of particular interest as it has been shown to be downregulated in breast cancer cell lines (34) and the gene for 14-3-3σ/Sfn is located in the distal arm of mouse chromosome 4, a region of recurrent loss in KI mammary tumors (17, 31). TM15 cells, which do not express detectable levels of endogenous 14-3-3σ, were infected with retrovirally expressed 14-3-3σ, and stable cell lines were generated. To examine whether EGR2 and 14-3-3σ interact, immunoprecipitations for 14-3-3σ were performed with lysates from the 14-3-3σ-stable TM15 cells. The immunoprecipitated proteins were demonstrated to contain EGR2, arguing that EGR2 and 14-3-3σ interact (Fig. 5A). To determine whether the association is dependent on phosphorylation of EGR2 at serine 376, a cDNA encoding a mutated form of EGR2 was generated in which serine 376 was replaced with an alanine (EGR2-S376A). Coexpression of EGR2-S376A and 14-3-3σ in 293T cells, followed by immunoprecipitation of the lysates with either a V5-specific antibody to tagged EGR2-S376A or a 14-3-3σ-specific antibody did not reveal an association between EGR2-S376A

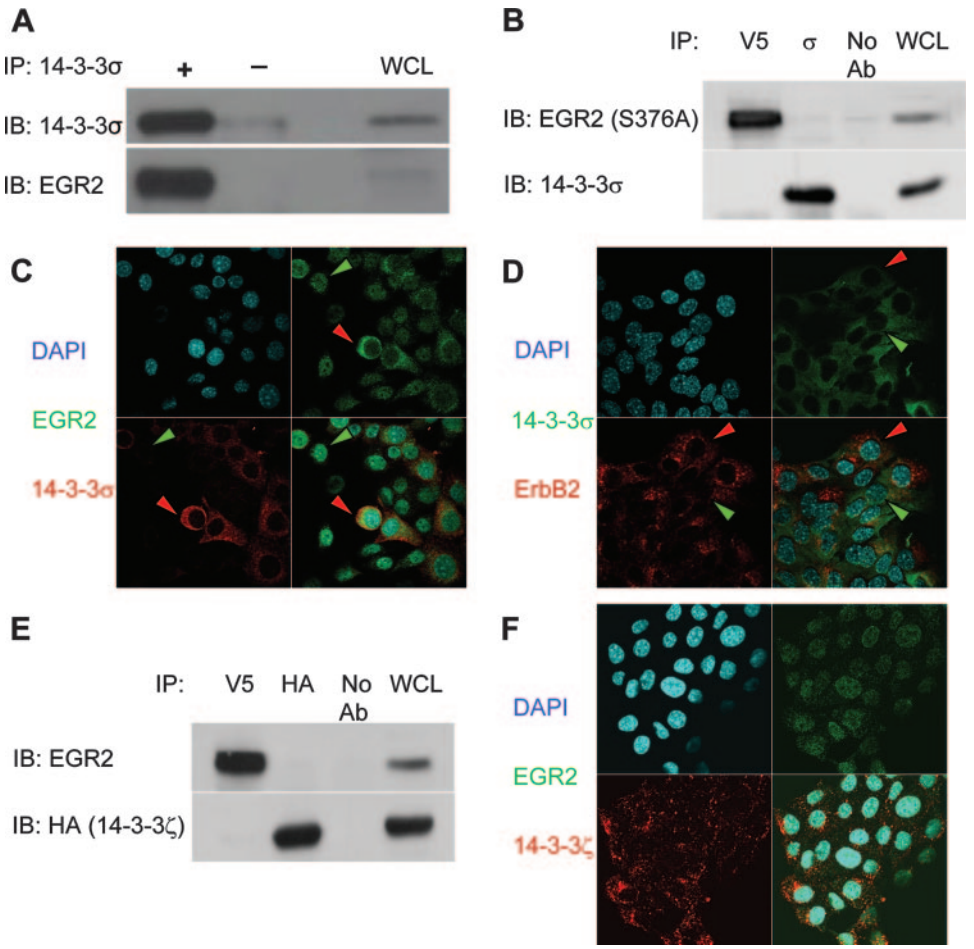

FIG. 5. 14-3-3σ overexpression leads to a decrease in ErbB2 levels and results in relocalization of EGR2 to the cytoplasm. (A) 14-3-3σ was immunoprecipitated (IP) from lysates of TM15 cells stably expressing 14-3-3σ, and the precipitated proteins were resolved by SDS-PAGE and immunoblotted (IB) for EGR2. WCL, whole-cell lysate. (B) Lysates of 293T cells cotransfected with EGR2-S376A-V5 and 14-3-3σ were immunoprecipitated with V5- and 14-3-3σ-specific antibodies (Ab). The isolated complexes were blotted for EGR2 (top) or 14-3-3σ (bottom). (C) 14-3-3σ (red) and EGR2 (green). Note the nucleus-localized EGR2 in cells expressing low levels of 14-3-3σ (green arrowheads) and the cytoplasmic EGR2 in the high-14-3-3σ-expressing cells (red arrowheads). (D) 14-3-3σ (green) and ErbB2 (red). Note the low ErbB2 levels in cells expressing high levels of 14-3-3σ (green arrowheads), whereas cells with low 14-3-3σ levels have high ErbB2 expression (red arrowheads). (E) Lysates of 293T cells cotransfected with EGR2-V5 and HA–14-3-3ζ were immunoprecipitated with V5- and HA-specific antibodies. The isolated complexes were blotted for EGR2 (top) or HA (bottom). (F) TM15 cells stably expressing HA–14-3-3ζ were stained with antibodies to HA (red) and EGR2 (green). Note that EGR2 remains nucleus localized in the presence of high levels of 14-3-3ζ.

and 14-3-3σ (Fig. 5B). This argues that phosphorylation of EGR2 at serine 376 is required for 14-3-3σ binding. Immunofluorescent staining and confocal microscopy of TM15 cells stably expressing 14-3-3σ revealed a relocalization of EGR2 from the nucleus to the cytoplasm, whereas EGR2 remained nucleus localized in cells expressing undetectable to low levels of 14-3-3σ (Fig. 5C). The nuclear localization of EGR2 in the low-14-3-3σ-expressing cells was identical to the staining pattern observed in the parental TM15 cell line (data not shown). Furthermore, the overexpression of 14-3-3σ resulted in decreased ErbB2 expression in the cells in which 14-3-3σ levels were high compared to cells expressing low or undetectable levels of 14-3-3σ (Fig. 5D). We then addressed whether the relocalization of EGR2 and downregulation of ErbB2 levels are attributable to other 14-3-3 family members. We first examined whether the related 14-3-3ζ isoform is capable of associating with EGR2. Cotransfection of EGR2 and 14-3-3ζ, followed by reciprocal immunoprecipitations, revealed that the 14-3-3ζ isoform does not associate with EGR2 (Fig. 5E). Furthermore, the stable expression of 14-3-3ζ in TM15 cells did not affect the localization of EGR2, whereby EGR2 remained nucleus localized in 14-3-3ζ-expressing cells (Fig. 5F). Collectively, the results suggest that 14-3-3σ sequesters EGR2 in the cytoplasm in a phosphorylation-dependent manner, leading to a downregulation of ErbB2 levels.

DISCUSSION

The ability of EGR2 to regulate *erbB2* expression is particularly compelling in that EGR2 and ErbB2 exhibit overlapping expression patterns during embryonic development (14). Additionally, it has been shown that ablation of ErbB2 or EGR2 function in neural tissue is associated with a similar myelination defect (14, 32). More recently, we have demonstrated that

a muscle-specific deletion of ErbB2 results in a spindle cell defect (2) that is identical to that observed in mice lacking the EGR2 family member EGR3 (47). Finally, expression of EGR1 has been implicated in the upregulation of EGFR in response to hypoxia (35). Together, these observations suggest that the EGR transcription factors may play a critical role in regulating the expression of the EGFR family.

A potential genetic link between CITED1 and ErbB2 is also suggested. CITED1-null mice display a mammary gland ductal outgrowth defect (18) that is akin to the phenotype seen upon mammary tissue-specific deletion of ErbB2 (4). Furthermore, during pubertal mammary gland development, the CITED1 expression levels were shown to parallel that of the EGFR ligand amphiregulin, and microarray analysis of CITED1-null mammary glands revealed a downregulation of amphiregulin (18). The potential role of CITED1 in upregulating amphiregulin suggests another mechanism by which CITED1 can potentiate ErbB2 signaling, in addition to transcriptional regulation of *erbB2* expression. It is interesting that the WT1 transcription factor that is closely related to the EGR family has been shown to transcriptionally activate amphiregulin gene expression (28). It this regard, it would be interesting to explore whether EGR2 may also be involved in the regulation of amphiregulin, which may represent another example of gene coregulation with CITED1.

The upregulation of EGR2 and CITED1 in this unique ErbB2 model raises the intriguing possibility that the upregulation of EGR2 and CITED1 may be an important event in the induction of human breast cancer. Conceivably in concert with gene amplification, elevation of these key transcription factors may allow cells to attain a threshold of ErbB2 expression required for the induction of cellular transformation. The observation that EGR2 is capable of upregulating ErbB2 expression in different cancer cell types also has important implications in understanding the selection of genetic events in tumor progression. Furthermore, elevated EGR2 expression has previously been detected in ErbB2-expressing breast cancer cell lines (44). It is therefore conceivable that the transcriptional upregulation of ErbB2 by EGR2 may represent a positive feedback loop. Although EGR2 has not been extensively examined for its role in tumorigenesis, one study has suggested that EGR2 may be important for the growth-suppressive effects of PTEN. EGR2 expression was shown to decrease colony formation in two endometrial cancer cell lines, an ovarian cancer cell line, and two colon cancer cell lines (50). Further studies demonstrated that EGR2 induced apoptosis in cancer cell lines and was able to activate the transcription of BNIP3L and BAK (49). The EGR2 family member EGR1 has been more extensively studied in terms of tumorigenesis and has been shown to play opposing roles in cancer. Decreased EGR1 expression has been demonstrated in cancers of the breast (19), lung (29), skin, liver, and esophagus (16), but increased expression has been noted in malignancies of the stomach (25), colon and rectum (48), and prostate (12). Given the high sequence identity between EGR1 and EGR2, it is likely that EGR2 will also prove to have multiple functions in tumorigenesis that are cell type and tissue context dependent. Although this represents the first report implicating CITED1 in *erbB2* expression in breast cancer, CITED1 has previously been implicated as a potent coactivator of ERα in MCF-7 breast cancer cells (53).

Here we have shown that expression of the 14-3-3σ tumor suppressor results in the sequestration of EGR2 from the nucleus to the cytoplasm (Fig. 5). We have further demonstrated that the relocalization of EGR2 from the nucleus to the cytoplasm is correlated with a reduction of ErbB2 expression in mammary tumor cells (Fig. 5). Given the fact that a large percentage of human breast cancers and their derived cell lines exhibit a loss of 14-3-3σ expression (17, 34), one of the molecular explanations for the selective loss of 14-3-3σ expression is to allow the recruitment of the EGR2/CITED1 complex to its transcriptional targets. Indeed, the majority of KI tumors and ErbB2-derived human breast cancer cell lines that lack 14-3-3σ expression have elevated ErbB2 expression (34). Although the downregulation of 14-3-3σ may provide a mechanism for promoting tumor development in allowing the EGR2/CITED1 complex to activate *erbB2* expression, it is by no means the only mechanism by which the loss of 14-3-3σ impacts on tumor progression. It has recently been demonstrated that 14-3-3σ plays an important role in mitotic translation. It was shown that cells deficient in 14-3-3σ lack the ability to stimulate cap-independent translation and do not suppress cap-dependent translation, leading to impaired mitosis (51). It therefore appears that 14-3-3σ has a number of different functions in the normal cell and that its deletion may lead to oncogenesis. Future studies directed toward elucidating the relative contribution of the EGR2/CITED1 complex to the induction of ErbB2-positive breast cancer may provide important insights into the development of therapeutic targets for the treatment of this prevalent but poorly understood disease.

ACKNOWLEDGMENTS

This research was funded by National Cancer Institute of Canada/Canadian Breast Cancer Research Alliance grant 015120 (to W.J.M.), Canadian Institutes of Health Research grant MOP-10594 (to W.J.M.), and U.S. Department of Defence Breast Cancer Research Initiative grant W81XWH-05-1-0405 (to W.J.M.). R.L.D. was supported by studentships from the McGill University Health Center, NSERC, and a predoctoral research scholarship from the U.S. Department of Defense Breast Cancer Research Initiative (W81XWH-04-1-0363). C.L. was supported by a predoctoral research scholarship from the U.S. Department of Defense Breast Cancer Research Initiative (W81XWH-06-1-0700). W.J.M. is supported by a CRC chair in Molecular Oncology.

REFERENCES

1. **Andrechek, E., M. Laing, A. Girgis-Gabardo, P. Siegel, R. Cardiff, and W. Muller.** 2003. Gene expression profiling of Neu-induced mammary tumors from transgenic mice reveals genetic and morphological similarities to ErbB-2 expressing human breast cancers. Cancer Res. **63:**4920–4926.
2. **Andrechek, E. R., W. R. Hardy, A. A. Girgis-Gabardo, R. L. Perry, R. Butler, F. L. Graham, R. C. Kahn, M. A. Rudnicki, and W. J. Muller.** 2002. ErbB2 is required for muscle spindle and myoblast cell survival. Mol. Cell. Biol. **22:**4714–4722.
3. **Andrechek, E. R., W. R. Hardy, P. M. Siegel, M. A. Rudnicki, R. D. Cardiff, and W. J. Muller.** 2000. Amplification of the neu/erbB-2 oncogene in a mouse model of mammary tumorigenesis. Proc. Natl. Acad. Sci. USA **97:** 3444–3449.
4. **Andrechek, E. R., D. White, and W. J. Muller.** 2005. Targeted disruption of ErbB2/Neu in the mammary epithelium results in impaired ductal outgrowth. Oncogene **24:**932–937.
5. **Benz, C. C., R. C. O'Hagen, B. Ritcher, G. K. Scott, C.-H. Chang, X. Xiong, K. Chew, B.-M. Ljung, S. Edgerton, A. Thor, and J. A. Hassell.** 1997. HER2/Neu and the Ets transcription activator PEA3 are coordinately upregulated in human breast cancer. Oncogene **15:**1513–1525.
6. **Bosher, J., N. F. Totty, J. J. Hsuan, T. Williams, and H. C. Hurst.** 1996. A family of AP-2 proteins regulates c-erbB-2 expression in mammary carcinoma. Oncogene **13:**1701–1707.
7. **Bosher, J., T. Williams, and H. Hurst.** 1995. The developmentally regulated

transcription factor AP-2 is involved in c-erbB-2 overexpression in human mammary carcinoma. Proc. Natl. Acad. Sci. USA **92:**744–747.
8. **Bouchard, L., L. Lamarre, P. J. Tremblay, and P. Jolicoeur.** 1989. Stochastic appearance of mammary tumors in transgenic mice carrying the MMTV/c-neu oncogene. Cell **57:**931–936.
9. **Chang, C.-H., G. K. Scott, W.-L. Kuo, X. Xiong, Y. Suzdaltseva, J. W. Park, P. Sayre, K. Erny, C. Collins, G. W. Gray, and C. C. Benz.** 1997. ESX: a structurally unique Ets overexpressed early during human breast tumorigenesis. Oncogene **14:**1617–1622.
10. **Chavrier, P., U. Janssen-Timmen, M. G. Mattei, M. Zerial, R. Bravo, and P. Charnay.** 1989. Structure, chromosome location, and expression of the mouse zinc finger gene Krox-20: multiple gene products and coregulation with the proto-oncogene c-*fos*. Mol. Cell. Biol. **9:**787–797.
11. **Dougall, W. C., X. Qian, N. C. Peterson, M. J. Miller, A. Samanta, and M. I. Greene.** 1994. The neu-oncogene: signal transduction pathways, transformation mechanisms and evolving therapies. Oncogene **9:**2109–2123.
12. **Eid, M. A., M. V. Kumar, K. A. Iczkowski, D. G. Bostwick, and D. J. Tindall.** 1998. Expression of early growth response genes in human prostate cancer. Cancer Res. **58:**2461–2468.
13. **Garcia-Dominguez, M., P. Gilardi-Hebenstreit, and P. Charnay.** 2006. PIASxβ acts as an activator of *Hoxb1* and is antagonized by Krox20 during hindbrain segmentation. EMBO J. **25:**2432–2442.
14. **Garratt, A., O. Voiculescu, P. Topilko, P. Charnay, and C. Birchmeier.** 2000. A dual role of erbB2 in myelination and in expression of the Schwann cell precursor pool. J. Cell Biol. **148:**1035–1046.
15. **Guy, C. T., M. A. Webster, M. Schaller, T. J. Parsons, R. D. Cardiff, and W. J. Muller.** 1992. Expression of the neu protooncogene in the mammary epithelium of transgenic mice induces metastatic disease. Proc. Natl. Acad. Sci. USA **89:**10578–10582.
16. **Hao, M. W., Y. R. Liang, Y. F. Liu, L. Liu, M. Y. Wu, and H. X. Yang.** 2002. Transcription factor EGR-1 inhibits growth of hepatocellular carcinoma and esophageal carcinoma cell lines. World J. Gastroenterol. **8:**203–207.
17. **Hodgson, J. G., T. Malek, S. Bornstein, S. Hariono, D. G. Gidzinger, W. J. Muller, and J. W. Gray.** 2005. Copy number aberrations in mouse breast tumors reveal loci and genes important in tumorigenic receptor tyrosine kinase signaling. Cancer Res. **65:**9695–9704.
18. **Howlin, J., J. McBryan, S. Napoletano, T. Lambe, E. McArdle, T. Shioda, and F. Martin.** 2006. CITED1 homozygous null mice display aberrant pubertal mammary ductal morphogenesis. Oncogene **25:**1532–1542.
19. **Huang, R. P., Y. Fan, I. de Belle, C. Neimeyer, M. M. Gottardis, D. Mercola, and E. D. Adamson.** 1997. Decreased Egr-1 expression in human, mouse and rat mammary cells and tissues correlates with tumor formation. Int. J. Cancer **72:**102–109.
20. **Hynes, N., H. Gerber, S. Saurer, and B. Groner.** 1989. Overexpression of the c-erbB-2 protein in human breast tumor cell lines. J. Cell. Biochem. **39:**167–183.
21. **Hynes, N. E., and D. F. Stern.** 1994. The biology of erbB-2/neu/HER-2 and its role in cancer. Biochim. Biophys. Acta **1198:**165–184.
22. **Kaya, H., T. Ragazzini, E. Aribal, I. Guney, and E. Kotiloglu.** 2001. Her-2/neu gene amplification compared with HER-2/neu protein overexpression on ultrasound guided core-needle biopsy specimens of breast carcinoma. Pathol. Oncol. Res. **7:**279–283.
23. **King, C., M. Kraus, and S. A. Aaronson.** 1985. Amplification of a novel v-erbB-related gene in human mammary carcinoma. Science **229:**974–976.
24. **King, C., S. Swain, L. Porter, S. Steinberg, M. Lippman, and E. Gelman.** 1989. Heterogeneous expression of erbB-2 messenger RNA in human breast cancer. Cancer Res. **49:**4185–4191.
25. **Kobayashi, D., M. Yamada, C. Kamagata, R. Kaneko, N. Tsuji, M. Nakamura, A. Yagihashi, and N. Watanabe.** 2002. Overexpression of early growth response-1 as a metastasis-regulatory factor in gastric cancer. Anticancer Res. **22:**3963–3970.
26. **Kraus, M., N. Popescu, C. Amsbaugh, and C. King.** 1987. Overexpression of the EGF receptor-related proto-oncogene erbB-2 in human mammary tumor cell lines by different molecular mechanisms. EMBO J. **6:**605–610.
27. **LeBlanc, S. E., S.-W. Jang, R. M. Ward, L. Wrabetz, and J. Svaren.** 2006. Direct regulation of myelin protein zero expression by the Egr2 transactivator. J. Biol. Chem. **281:**5453–5460.
28. **Lee, S. B., K. Huang, R. Palmer, V. B. Truong, D. Herzlinger, K. A. Kolquist, J. Wong, C. Paulding, S. K. Yoon, W. Gerald, J. D. Oliner, and D. A. Haber.** 1999. The Wilms tumor suppressor WT1 encodes a transcriptional activator of amphiregulin. Cell **98:**663–673.
29. **Levin, W. J., M. F. Press, R. B. Gaynor, V. P. Sukhatme, T. C. Boone, P. T. Reissmann, R. A. Figlin, E. C. Holmes, L. M. Souza, and D. J. Slamon.** 1995. Expression patterns of immediate early transcription factors in human non-small cell lung cancer. Oncogene **11:**1261–1269.
30. **Manzanares, M., J. Nardelli, P. Gilardi-Hebenstreit, H. Marshall, F. Guidicelli, M. T. Martinez-Pastor, R. Krumlauf, and P. Charnay.** 2002. Krox20 and kreisler co-operate in the transcriptional control of segmental expression of *Hoxb3* in the developing hindbrain. EMBO J. **21:**365–376.
31. **Montagna, C., E. Andrechek, H. Padilla-Nash, W. Muller, and T. Ried.** 2002. Centrosome abnormalities, recurring deletions of chromosome 4, and genomic amplification of HER2/neu define mouse mammary gland adenocarcinomas induced by mutant HER2/neu. Oncogene **21:**890–898.
32. **Nagarajan, R., J. Svaren, N. Le, T. Araki, M. Watson, and J. Milbrandt.** 2001. EGR2 mutations in inherited neuropathies dominant-negatively inhibit myelin gene expression. Neuron **30:**355–368.
33. **Nair, S. S., V. A. Chaubal, T. Shioda, K. R. Coser, and M. Mojamdar.** 2001. Over-expression of MSG1 transcriptional co-activator increases melanin in B16 melanoma cells: a possible role for MSG1 in melanogenesis. Pigment Cell Res. **14:**206–209.
34. **Neve, R. M., K. Chin, J. Fridlyand, J. Yeh, F. L. Baehner, T. C. L. Fevr, N. Bayani, J. P. Coppe, F. Tong, T. Speed, P. T. Spellman, S. DeVries, A. Lapuk, N. J. Wang, W. L. Kuo, J. L. Stilwell, D. Pinkel, D. G. Albertson, F. M. Waldman, F. McCormick, R. B. Dickson, M. D. Johnson, M. Lippman, S. Ethier, A. Gazdar, and J. W. Gray.** 2006. A collection of breast cancer cell lines for the study of functionally distinct cancer subtypes. Cancer Cell **10:**515–527.
35. **Nishi, H., K. H. Nishi, and A. C. Johnson.** 2002. Early growth response gene-1 mediates up-regulation of epidermal growth factor receptor during hypoxia. Cancer Res. **62:**827–834.
36. **Nonchev, S., C. Vesque, M. Maconochie, T. Seitanidou, L. Ariza-McNaughton, M. Frain, H. Marshall, M. H. Sham, R. Krumlauf, and P. Charnay.** 1996. Segmental expression of Hoxa-2 in the hindbrain is directly regulated by Krox-20. Development **122:**543–554.
37. **Nonchev, S., M. Maconochie, C. Vesque, S. Aparicio, L. Ariza-McNaughton, M. Manzanares, K. Maruthainar, A. Kuroiwa, S. Brenner, P. Charnay, and R. Krumlauf.** 1996. The conserved role of Krox-20 in directing Hox gene expression during vertebrate hindbrain segmentation. Proc. Natl. acad. Sci. USA **93:**9339–9345.
38. **Patten, B. A., J. M. Peyrin, G. Weinmaster, and G. Corfas.** 2003. Sequential signaling through Notch1 and erbB receptor mediates radial glia differentiation. J. Neurosci. **23:**6132–6140.
39. **Scott, G. K., C.-H. Chang, K. M. Erny, F. Xu, W. J. Fredericks, F. J. Rauscher III, A. D. Thor, and C. C. Benz.** 2000. Ets regulation of the *erbB2* promoter. Oncogene **19:**6490–6502.
40. **Shioda, T., M. H. Fenner, and K. J. Isselbacher.** 1996. Msg1, a novel melanocyte-specific gene, encodes a nuclear protein and is associated with pigmentation. Proc. Natl. Acad. Sci. USA **93:**12298–12303.
41. **Siegel, P. M., E. D. Ryan, R. D. Cardiff, and W. J. Muller.** 1999. Elevated expression of activated forms of Neu/ErbB-2 and ErbB-3 are involved in the induction of mammary tumors in transgenic mice: implications for human breast cancer. EMBO J. **18:**2149–2164.
42. **Slamon, D., W. Godolphin, L. Jones, J. Holt, S. Wong, D. Keith, W. Levin, S. Stuart, J. Udove, and A. Ullrich.** 1989. Studies of the HER-2/neu protooncogene in human breast cancer and ovarian cancer. Science **244:**707–712.
43. **Slamon, D. J., G. M. Clark, S. G. Wong, W. J. Levin, A. Ullrich, and W. L. McGuire.** 1987. Human breast cancer: correlation of relapse and survival with amplification of the HER-2/neu oncogene. Science **235:**177–182.
44. **Sweeney, C., D. Fambrough, C. Huard, A. J. Diamonti, E. S. Lander, L. C. Cantley, and K. L. Carraway III.** 2001. Growth factor-specific signaling pathway stimulation and gene expression mediated by ErbB receptors. J. Biol. Chem. **276:**22685–22698.
45. **Swirnoff, A. H., and J. Milbrandt.** 1995. DNA-binding specificity of NGFI-A and related zinc finger transcription factors. Mol. Cell. Biol. **15:**2275–2287.
46. **Theil, T., M. Frain, P. Gilardi-Hebenstreit, A. Flenniken, P. Charnay, and D. G. Wilkinson.** 1998. Segmental expression of the EphA4 (Sek-1) receptor tyrosine kinase in the hindbrain is under direct transcriptional control of Krox-20. Development **125:**443–452.
47. **Tourtellotte, W. G., and J. Milbrandt.** 1998. Sensory ataxia and muscle spindle agenesis in mice lacking the transcription factor Egr3. Nat. Genet. **20:**87–91.
48. **Tsunoda, T., Y. Koh, F. Koizumi, S. Tsukiyama, H. Ueda, F. Taguchi, H. Yamaue, N. Saijo, and K. Nishio.** 2003. Differential gene expression profiles and identification of the genes relevant to clinicopathologic factors in colorectal cancer selected by cDNA array method in combination with principal component analysis. Int. J. Oncol. **23:**49–59.
49. **Unoki, M., and M. Nakamura.** 2003. EGR2 induces apoptosis in various cancer cell lines by direct transactivation of BNIP3L and BAK. Oncogene **22:**2172–2185.
50. **Unoki, M., and M. Nakamura.** 2001. Growth-suppressive effects of BPOZ and EGR2, two genes involved in the PTEN signaling pathway. Oncogene **20:**4457–4465.
51. **Wilker, E. W., M. A. van Vugt, S. A. Artim, P. H. Huang, C. P. Petersen, H. C. Reinhardt, Y. Feng, P. A. Sharp, N. Sonenberg, F. M. White, and M. B. Yaffe.** 2007. 14-3-3σ controls mitotic translation to facilitate cytokinesis. Nature **446:**329–332.
52. **Yahata, T., M. P. de Caestecker, R. J. Lechleider, S. Andriole, A. B. Roberts, K. J. Isselbacher, and T. Shioda.** 2000. The MSG1 non-DNA-binding transactivator binds to the p300/CBP coactivators, enhancing their functional link to the Smad transcription factors. J. Biol. Chem. **275:**8825–8834.
53. **Yahata, T., W. Shao, S. Endoh, J. Hur, K. R. Coser, H. Sun, Y. Ueda, S. Kato, K. J. Isselbacher, M. Brown, and T. Shioda.** 2001. Selective coactivation of estrogen-dependent transcription by CITED1 CBP/p300-binding protein. Genes Dev. **15:**2598–2612.